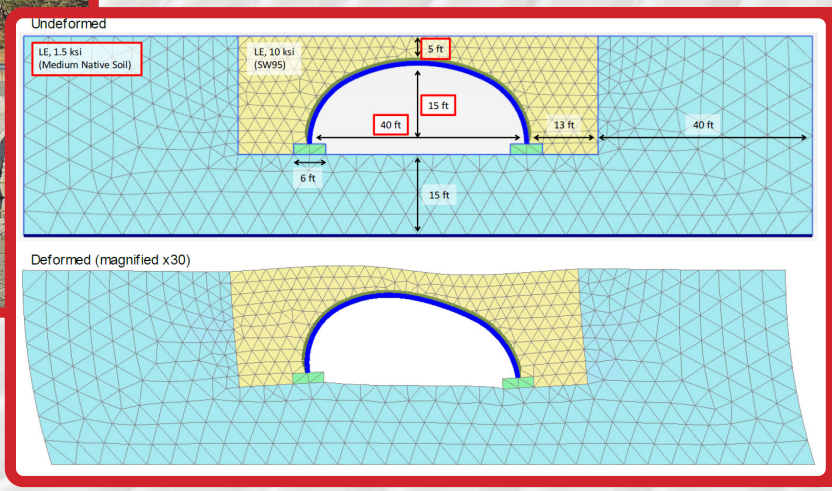

National Corrugated Steel Pipe Association Presents

Development of Seismic Analysis Procedure for Corrugated Metal Buried Structures

May 2024

CONTECH ENGINEERED SOLUTIONS

LANE

American Iron and Steel Institute

SGH

EXECUTIVE SUMMARY

Current codes do not require detailed seismic design of buried structures such as culverts or buried bridges based largely on historical performance relative to above-ground structures. For installations where explicit design for seismic demands is required by local provisions or for life safety, the current standard of practice requires detailed finite element analysis, for which there is no standard procedure. Previous research developed a simplified seismic analysis approach for rigid box structures and simplified closed-form seismic demand equations for rigid and flexible circular pipes, but no simplified design method exists for use with typical geometries of buried large-span corrugated metal arches on footings.

This report details development of closed-form equations to estimate seismic demand due to lateral accelerations on typical arch-shaped corrugated metal buried structures based on the results of detailed parametric finite element analyses. These equations are intended to allow for simple screening of seismic demands and are developed to be consistent with the existing AASHTO design methods for these structures. The equations replace the need to complete two-dimensional dynamic or pseudo-static soil-structure interaction (SSI) finite element analyses (FEA) for typical structures.

The recommended equations are as follows:

$$T = \left(\frac{H^{0.6}}{{M_s}^{0.33}}\right) * 2 * R * S * k_h$$

$$M = \left(\frac{I * (R + 60)^4}{2975 * {M_s}^{0.1}} + 80\right) * k_h$$

where:

T = unfactored seismic design thrust (lbf/in.)
M = unfactored seismic design moment (lbf-in./in.)
I = profile moment of inertia (in^4/in.)
R = structure rise (ft)
S = structure span (ft)
H = fill depth over top of structure (ft)
M_s = constrained modulus of native soil (ksi)
k_h = seismic lateral acceleration coefficient (g) per AASHTO Section 11.6.5.2.2

The thrust equation ranges from 10% unconservative to 34% conservative. The moment equation ranges from 5% unconservative to 47% conservative.

These equations are applicable to typical structures and typical installations meeting the following tabulated conditions. Note that the embedment material should be considered as SW soils with 85% compaction or greater or ML soils with 95% compaction or greater. Installations outside these conditions still require FEA to determine seismic demands.

Parameter	Min	Max
Span (ft)	20	60
Rise (ft)	10	40
Fill depth (ft)	2	10
Profile	6x2	15x5.5
Thickness (GA)	1	8
Structure Material	Steel, Aluminum	
Native soil (M_s = constrained modulus)	Poor (M_s = 0.8 ksi)	Good (M_s = 2.5 ksi)

Installations with larger structure span, deep cover, poor native soil, or high site seismicity are most likely to be controlled by seismic demand. The design equations may be overly conservative for installations in very good native soils, but seismic demands are unlikely to control design in these cases based on AASHTO load combinations. The design equations do not consider locations with faults, liquefaction, low-quality backfill, deep foundations, structure slopes, or surface ground slopes, which should be evaluated using SSI FEA based on the specific site conditions.

Appendix A provides a summary of relevant literature and current practice. Appendix B provides a design example demonstrating use of the equations. Appendix C details recommended changes to AASHTO to implement the equations. The following additional research is recommended to extend these findings.

- Extend comparison of pseudo-static acceleration and static racking approaches for modeling seismic demands in order to address variable preferences among researchers and reviewers.

- Investigate whether the Newmark reduction in lateral seismic acceleration detailed in NCHRP 611 for buried walls is appropriate for corrugated metal buried structures.
- Determine whether deep-corrugated buried structures can reliably retain static stability after plastic hinge formation, allowing design for flexural yielding under seismic loading.
- Evaluate variations in structural backfill width.
- Evaluate variations in backfill materials to include recycled backfill.
- Evaluate the effects of service deterioration (e.g. corrosion, foundation scour, etc…) on seismic demand.
- Obtain field measurements of recently installed larger span structures (within the past 15 years) that have been subjected to seismic loading and document performance, including comparisons with the proposed methodology.

Table of Contents

EXECUTIVE SUMMARY

CONTENTS **Page**

APPENDICES

1. BACKGROUND

1.1 Motivation

Buried structures have generally performed well in seismic events. In the 1989 Loma Prieta earthquake, the Alameda Highway Tunnel and BART subway system both sustained only minor damage, while several above-ground buildings and bridges sustained major damage [1, 2]. Isenberg [3] examined damaged steel buried structures from the 1965 Puget Sound, 1969 Santa Rosa, and 1971 San Fernando earthquakes, finding that all damage occurred at locations where severe corrosion had reduced capacity, and that uncorroded sections would have withstood the seismic loading. Youd and Beckman [4] inspected and reviewed performance of 17 corrugated metal buried structures with damage reported in the 1964 Alaska, 1971 San Fernando, 1983 Borah Peak, 1993 Hokkaido Nansi-Oki, and 1994 Northridge earthquakes, finding that all major damage was due to ground failure (e.g. liquefaction, slope instability, fault rupture) rather than lateral racking. A detailed literature review is provided in Appendix A.

Largely due to this strong performance record, national codes for design of buried structures typically do not require consideration of seismic demands. AASHTO LRFD Bridge Design Specifications (AASHTO) [5] Section 12.6.1 specifies that earthquake loads should be considered only where buried structures cross active faults, which is not common. State DOTs generally have not addressed seismic design of buried structures beyond referring to AASHTO specifications; however, some states are now examining this issue.

Study of recent large seismic events shows that buried structures are not immune from seismic damage. Davis and Bardet [6] examined over 60 corrugated metal buried structures near the epicenter of 1994 Northridge earthquake, finding that while smaller structures were undamaged, 10% of larger structures had significant damage ranging from residual lateral displacement to complete collapse. More significantly, the Dakai subway station collapsed in the 1995 Kobe earthquake due to lateral racking of the top slab away from end shear walls [7, 8].

Clearly, there are cases when seismic demand on buried structures should be considered in design. California and Washington, both seismically active states, require consideration of

seismic demands for buried structures with spans greater than 20 ft, such as buried bridges [9, 10]. Building code requirements for consideration of seismic demand generally extend to any structures with life-safety implications, which is increasingly applicable to buried structures that are being used for an expanding variety of applications.

The seismic behavior of buried structures is well-understood, both through theoretical work and physical testing, and has been documented in research by FHWA, PEER, Wang, Tohda, and Ulgen [11-15]. However, the current standard of practice for consideration of seismic demands on buried structures still requires detailed finite element analysis, which can be difficult to justify given that the previously described field experience shows that seismic demands rarely control service performance.

NCHRP 611 [16] developed a simplified analysis approach for buried concrete box structures, but this still requires an additional analysis model and is not applicable to flexible corrugated metal arch structures, which have fundamentally different seismic behavior. NCHRP 611 also proposed closed-form seismic demand equations for circular pipes, but these were not validated for other structural shapes.

1.2 Approach

This report describes the development of simplified, closed-form equations to estimate seismic demands due to lateral accelerations on commonly installed corrugated metal buried structures. These equations are intended to be compatible with the existing AASHTO design approach for these structures and will allow for quick screening of seismic demands without detailed finite element models. Vertical seismic accelerations are not considered herein since vertical accelerations are generally low when lateral accelerations are at their maximum, as discussed in AASHTO Article 11.6.5.2.1 and commentary.

A series of parametric finite element analysis (FEA) models were developed and analyzed using Plaxis 2D soil-structure interaction (SSI) software. We structured the FEA models to cover the range of typical arch-shaped structures and typical installations. The results of the

FEA models were studied to determine the impact of different variables on seismic demand and to determine a general form for closed-form demand equations. Conventional loadings such as soil load and live load, which have well-established design approaches in AASHTO, were not studied in this report. The equations were then calibrated to provide a reasonably conservative estimation of the seismic loading demands predicted by the FEA models.

This approach was selected to match approaches used to develop several existing AASHTO design equations for buried structures. The AASHTO equations used to calculate dead load moment demand in metal box culverts up to 36 ft span (Section 12.9.4.2) are based on calibration of polynomial equations to conservatively match FEA results [17]. Similarly, the equations used to determine global buckling capacity of deep corrugated structures (Section 12.8.9.6) are based on calibration of a best-fit curve to conservatively match experimental results [18]. Finally, the vertical arching factor equation used to calculate dead load demand in thermoplastic pipes (Section 12.12.3.5) is based on the adjustment of a theoretical equation to conservatively match FEA results [19].

2. SEISMIC STRUCTURAL ANALYSIS

2.1 Range of Installations Considered

Table 1 shows the range of parameters for typical installations of arch-shaped corrugated steel buried structures as determined in discussions with the National Corrugated Steel Pipe Association (NCSPA). Table 2 lists the FEA models run to cover the range of parameters and determine the effect of each parameter.

Table 1 – Range of Installation Parameters for Arch-Shaped Corrugated Steel Buried Structures

Parameter	Min	Max
Span (ft)	20	60
Rise (ft)	10	40
Fill depth (ft)	2	10
Profile	6x2	15x5.5
Thickness (GA)	1	8
Material	Steel	
Native soil (M_s = constrained modulus)	Poor (M_s = 0.8 ksi)	Good (M_s = 2.5 ksi)

Table 2 – FEA Model Matrix

Model	Span (ft)	Rise (ft)	Shape	Profile (in.)	GA	Native Soil	Fill Depth (ft)	k_h (g)
1	40	15	MR	15x5.5	5	Med	5	0.2
5	40	15	MR	15x5.5	1	Med	5	0.2
6	40	15	MR	15x5.5	8	Med	5	0.2
7	40	15	MR	15x5.5	5	High	5	0.2
8	40	15	MR	15x5.5	5	Low	5	0.2
10	40	15	MR	15x5.5	5	Med	5	0.4
11	40	15	MR	15x5.5	5	Med	3	0.2
12	40	15	MR	15x5.5	5	Med	10	0.2
13	60	20	MR	15x5.5	5	Med	5	0.2
14	23	11.5	MR	15x5.5	5	Med	5	0.2
15	23	11.5	MR	6x2	5	Med	5	0.2
16	40	10	LP	15x5.5	5	Med	5	0.2
17	40	30	HP	15x5.5	5	Med	5	0.2
18	40	10	BC	15x5.5	5	Med	5	0.2
20	40	15	MR	15x5.5	1	Low	5	0.2
21	40	15	MR	15x5.5	8	Low	5	0.2

MR = Multi-radius arch, LP = low-profile arch, HP = high-profile arch, BC = box culvert. GA = gauge thickness of corrugations, k_h = seismic lateral acceleration coefficient (see AASHTO Section 11.6.5.2.2).
Model numbers 2-4, 9, and 19 for investigation of modeling approach only, not used in equation optimization.

2.2 Model Details

Figure 1 shows a typical Plaxis 2D FEA model. The parameters outlined in red change between models, the other parameters are constant. All models use linear elastic soil material models, a linear elastic interface between the soil and structure with a modulus of approximately 10% of the stiffness of the embedment soil (900 psi), steel material for the structure, reinforced concrete strip footings, standard AASHTO embedment material and extents, soil unit weight of 120 pcf, and water table below the installation.

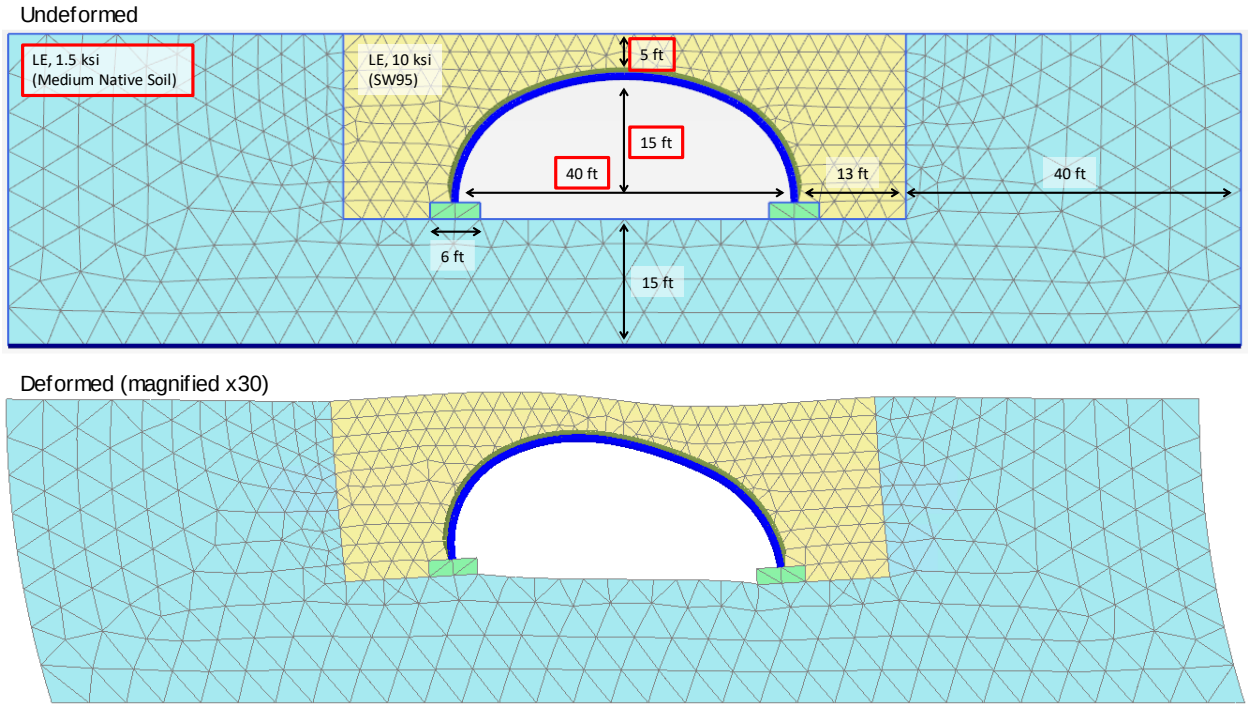

Figure 1 – Typical FEA Model (Model 1 Shown)

Linear elastic soil material models were used for consistency with previous research by Katona [20], Wang [13], and NCHRP 611 [16]. We set the stiffness of the embedment material to 10 ksi, based on the secant young's modulus for 10 psi confining pressure following the approach reported by Bowers, Webb, and Beaver [21] for SW100 material.

A representative interface reduction factor of 0.3 was selected to better capture the interaction between the soil and structure, mimicking a partial-slip condition. This results in a reduced interface Young's modulus of 900 psi. Previous research [13, 16] has assumed full-slip or no-slip

conditions between the soil and the structure, but the partial-slip condition represented by the reduced modulus is more realistic. For site-specific assessments, the use of a slip criterion (e.g., a friction coefficient of 0.3) is recommended to better capture the distribution of thrust around the circumference, rather than the reduced modulus approach which provides generalized behavior.

The base of the models was fixed against translation in all directions. Both vertical side boundaries are free laterally but fixed against vertical translation and the top boundary is free. Staged construction we used increments to isolate the effects of seismic load from the effects of dead load. Live load with the seismic load was not included.

Seismic loading was applied with a lateral pseudo-static acceleration equal to the design seismic lateral acceleration coefficient (force-based analysis). This matches the approach used in previous research by Wang [13] and NCHRP 611 [16]. Katona [20] validated a static racking approach, which requires imposing displacement at both vertical boundaries and the top boundary (deformation-based analysis). The static racking approach requires calculation of the imposed displacement based on the modulus of a single soil material. The approach used in this study accounts for the various different soil layers.

Figure 2 shows a comparison of seismic thrust and seismic bending moment demand generated in Model 1 using pseudo-static acceleration and static racking loading. Static racking demands are shown for runs with imposed displacement calculated based on the stiffness of the native soil and the stiffness of the embedment material.

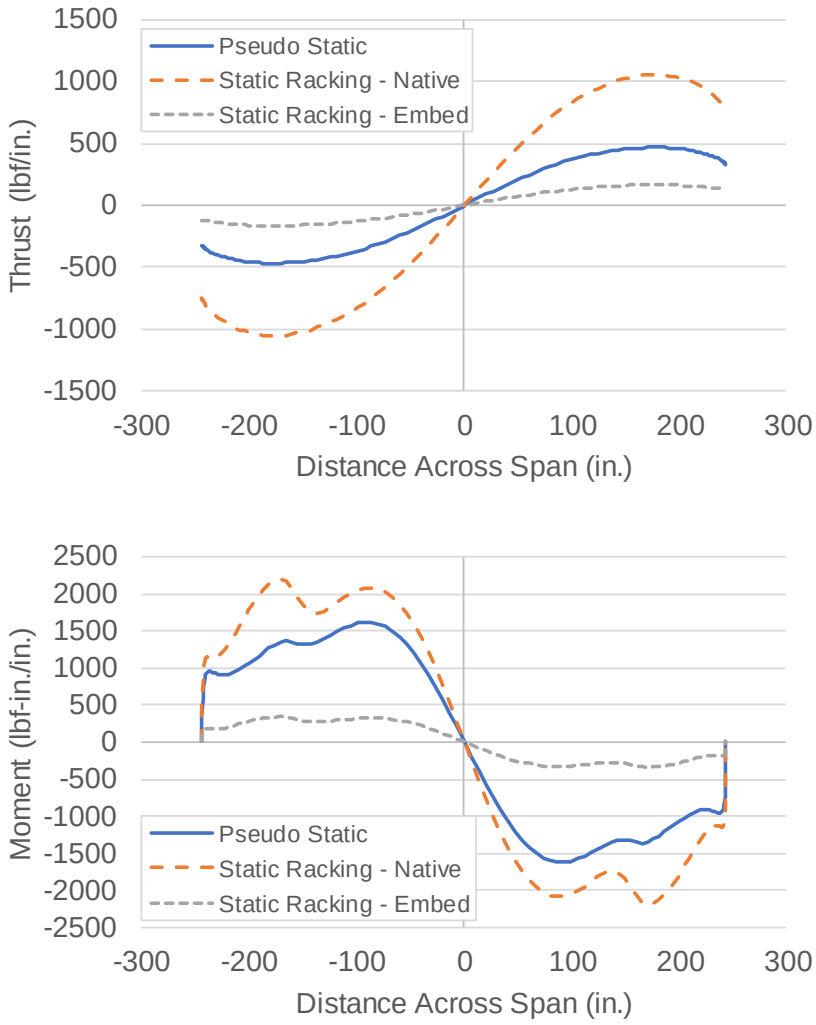

Figure 2 – Comparison of Pseudo-Static Acceleration and Static Racking Seismic Loading Approaches

The pseudo-static demands are bounded by the two static racking demands. The pseudo-static approach was used for consistency with the majority of the existing research, to capture the impact of both the native and embedment material, and to avoid potential issues with imposed displacements at the top boundary causing artificially high racking in models with shallow cover.

2.3 Model Results

The FEA results were evaluated comparatively to determine the effect of different variables on seismic demands. Figures 3-6 show the effects of structure stiffness, native soil stiffness, structure span, and structure shape, respectively. All plots show demand due to seismic loading only and do not include forces from dead or live loads.

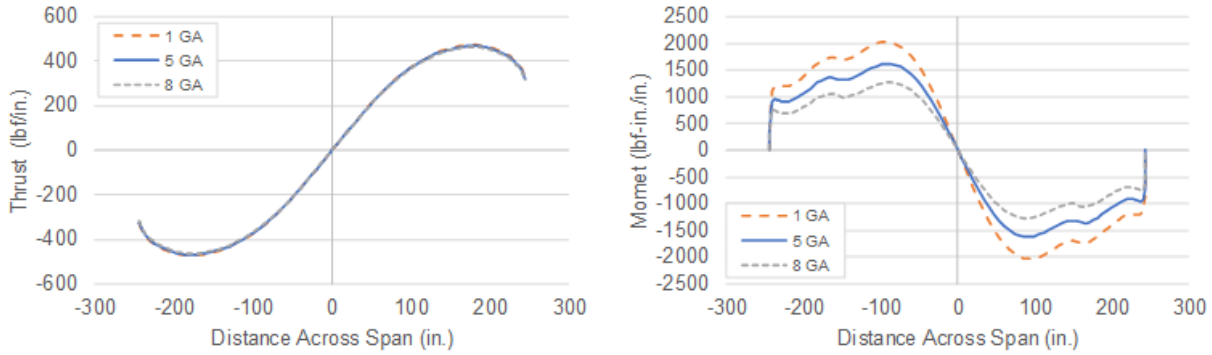

Figure 3 – Effect of Structure Stiffness on Seismic Demand

Figure 3 shows the effect of structure stiffness by comparing seismic demands from Models 1, 5, and 6, which have plate thickness of 5, 1, and 8 GA, respectively. Switching from 1 to 8 GA plate reduces the profile area by a factor of 1.67 from 4.63 in2/ft to 2.76 in2/ft but does not change the seismic thrust demand. The profile moment of inertia decreases by a factor of 1.68 from 1.47 in4/in to 0.875 in4/in and the seismic moment demand decreases by a factor of 1.61 from 2,032 lbf-in./in. to 1,265 lbf-in./in. indicating an approximately linear relationship.

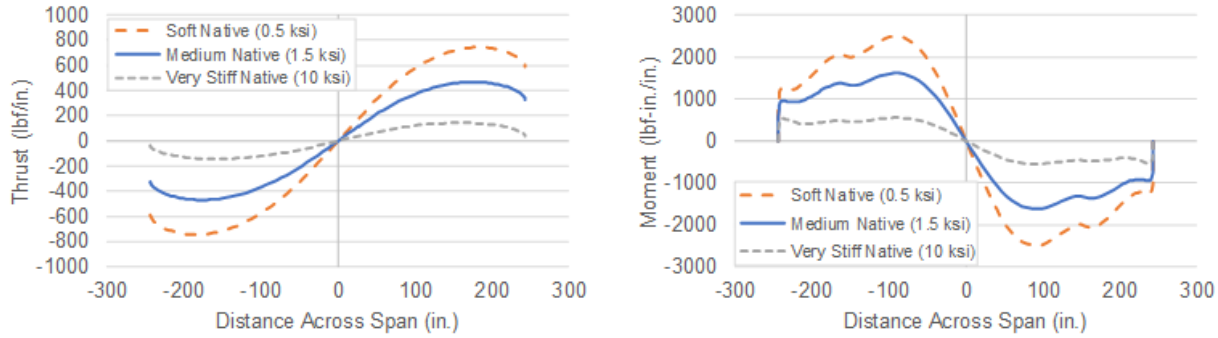

Figure 4 – Effect of Native Soil Stiffness on Seismic Demand

Figure 4 shows the effect of native soil stiffness by comparing seismic demands from Models 1, 7, and 8, which have native soil elastic modulus values of 1.5 ksi, 10 ksi, and 0.5 ksi, respectively. These elastic modulus values correspond to constrained modulus values of 2.41 ksi, 16.1 ksi, and 0.80 ksi, respectively, and shear modulus values of 0.56 ksi, 3.70 ksi, and 0.19 ksi, respectively, assuming a Poisson ratio of 0.35. Both seismic thrust and seismic moment demand show a non-linear relationship with the native soil stiffness.

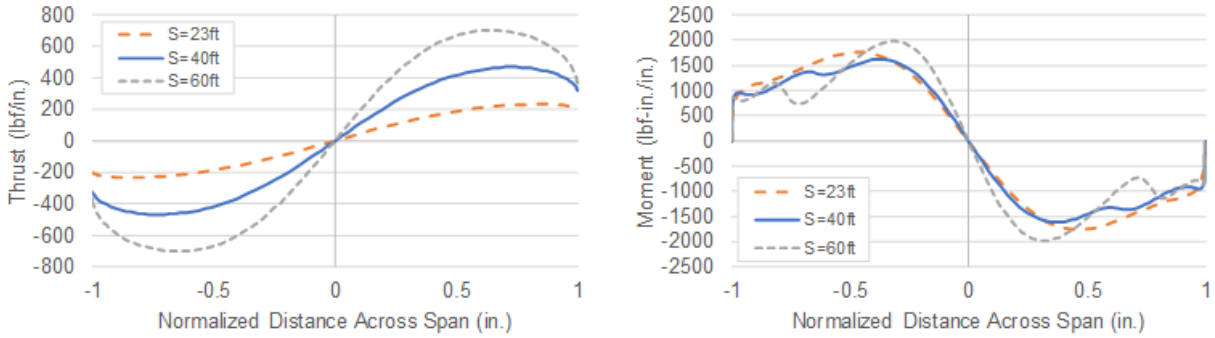

Figure 5 – Effect of Structure Span on Seismic Demand

Figure 5 shows the effect of structure span by comparing seismic demands from Models 1, 13, and 14 which are all multi-radius arch shapes but have spans of 40 ft, 60 ft, and 23 ft, respectively. Approximately tripling the structure span from 23 ft to 60 ft increases the seismic thrust demand from 233 lbf/in. to 702 lbf/in., a factor of 3.0, indicating an approximately linear relationship. However, the moment demand increases from 1759 lbf-in./in. to 1979 lbf-in./in., indicating a minor impact of span on seismic moment demand.

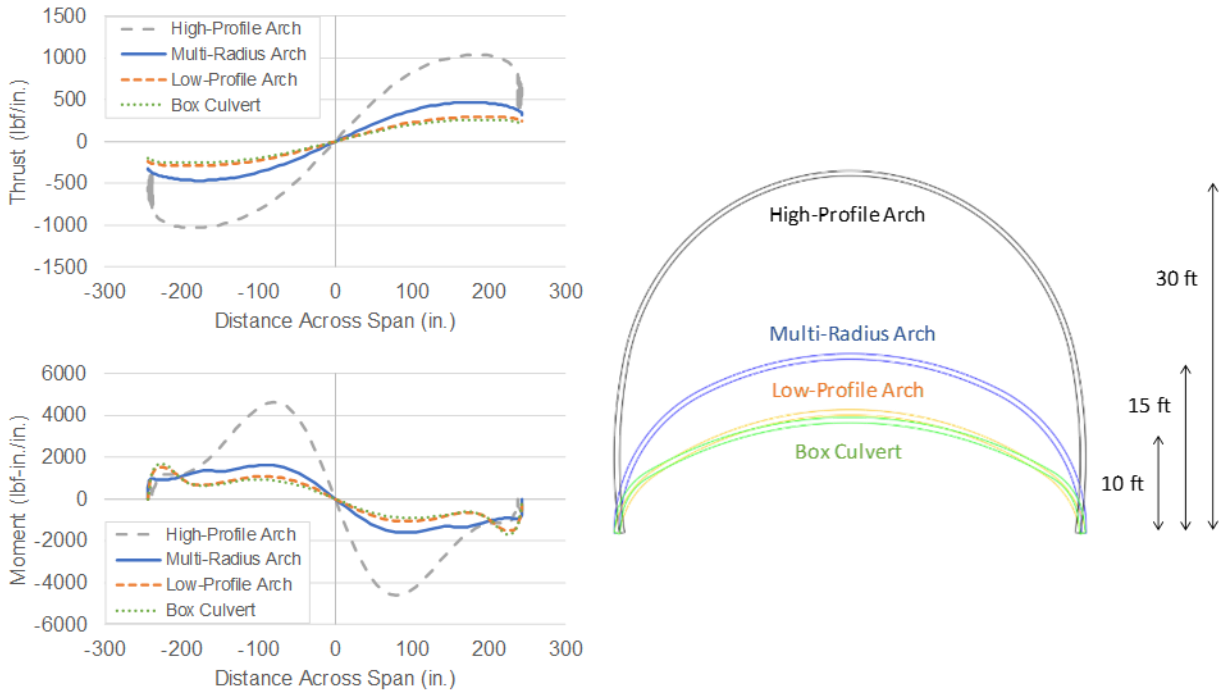

Figure 6 – Effect of Structure Shape on Seismic Demand

Figure 6 shows the effect of structure shape by comparing seismic demands from Models 1, 16, 17, and 18 which all have 40 ft span but are multi-radius arch, low-profile arch, high-profile arch, and box culvert shapes. The low-profile arch and box culvert both have a structure rise of 10 ft and have approximately equal seismic demands. The rise increases to 15 ft for the multi-radius arch and to 30 ft for the high-profile arch. Seismic thrust and moment both increase with rise, but the effect is approximately linear for thrust and non-linear for moment.

The effects observed from these comparisons and similar comparisons between other FEA models were used to develop the general form of seismic design equations.

3. DESIGN EQUATIONS

3.1 Applicability of Existing Equations

Before developing new equations, first it was confirmed that the existing closed-form equations developed in NCHRP 611 for seismic demand in circular pipes are not suitable for use with buried corrugated metal structures. Figure 7 compares seismic moment demands from the FEA models to seismic moment demands calculated with the NCHRP 611 circular pipe equations, using half the structure span as the radius in the equations.

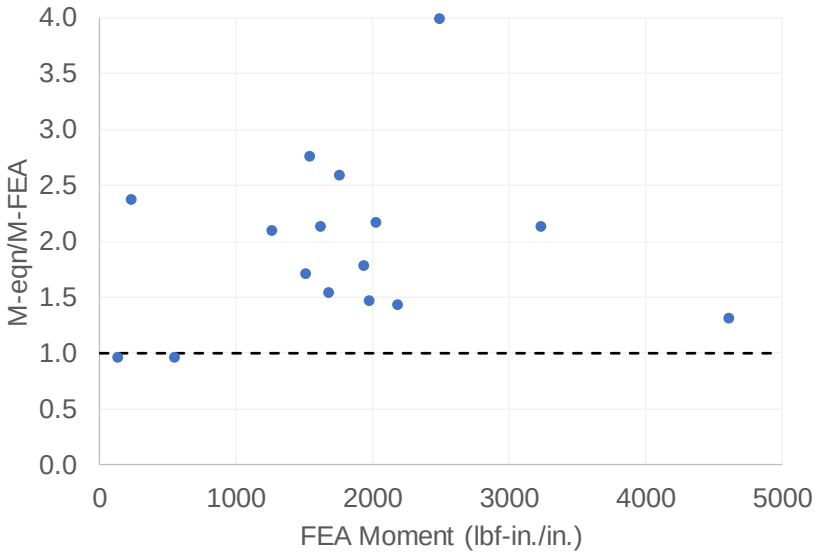

Figure 7 – Applicability of NCHRP 611 Circular Pipe Equations

Each point on the plot represents one FEA model from Table 2. The horizontal axis shows the maximum seismic moment in the structure from the FEA model. The vertical axis shows the ratio of the seismic moment predicted by the NCHRP 611 equation to the maximum seismic moment in the structure from the FEA model. A ratio greater than 1.0 indicates that the equation predicts higher seismic moment for that model.

The minimum, average, and maximum ratios are 0.96, 1.96, and 3.98, respectively. The NCHRP 611 equations developed for circular pipe significantly over-predict seismic moment demand when applied to buried arch-shaped corrugated metal structures.

3.2 General Form of Equations

Based on a comparative review of the FEA results, we developed the following general equations for seismic thrust and moment.

$$T = \left(\frac{H^{k_1}}{k_2 {M_s}^{k_3}} + k_4\right) * (R * S) * k_h$$

$$M = \left(\frac{I * (R + k_5)^{k_6}}{k_7 * {M_s}^{k_8}} + k_9\right) * k_h$$

where:

T = unfactored seismic design thrust (lbf/in.)
M = unfactored seismic design moment (lbf-in./in.)
I = profile moment of inertia (in^4/in.)
R = structure rise (ft)
S = structure span (ft)
H = fill depth over top of structure (ft)
M_s = constrained modulus of native soil (ksi)
k_h = seismic lateral acceleration coefficient (g) per AASHTO Section 11.6.5.2.2
$k_{1\text{-}9}$ = constant, factor, and exponent calibration terms for optimization

The variable effects discussed in Section 2.3 are reflected in the general form of the equations.

Area was not included in the thrust equation as structure hoop (axial) stiffness showed no effect on seismic thrust. We included profile moment of inertia as a linear term in the moment equation as structure bending stiffness showed a linear effect on seismic moment. We included structure span as a linear term in the thrust equation, but did not include it in the moment equation. We included structure rise as a linear term in the thrust equation and as a non-linear term in the moment equation.

3.3 Equation Optimization

The constant, factor, and exponent calibration terms were selected using particle swarm optimization (PSO). PSO is well-suited to problems with multiple variables and a wide range of possible solutions, such as these general equations. The details of the PSO approach are described by Keene and Beaver [22].

The PSO algorithm was set to find the calibration terms that produced the best average estimate of FEA demands from the equations. We constrained the algorithm such that 1) on average, the equation demands were conservative relative to the FEA demands, and 2) the equation demands were never more than 10% unconservative relative to any FEA demand. These constraints were selected to match the conservatism shown in the development of the other AASHTO FEA-based design equations discussed in Section 1.2, as shown in Table 3 below.

Table 3 – Conservatism of Existing AASHTO Design Equations

AASHTO Design Equation	AASHTO Section	Max Conservative	Max Unconservative
Moment Demand in Metal Box Culverts	12.9.4.2	40%	5%
Global Buckling of Deep Corrugated Structures	12.8.9.6	300%	2%
Vertical Arching Factor for Thermoplastic Pipe	12.12.3.5	50%	10%

3.4 Recommended Equations

Optimization of the general equations shown previously gives the following recommended equations for estimation of seismic thrust and moment demand for corrugated steel buried arch-shaped structures within the range of installation parameters shown in Table 1.

$$T = \left(\frac{H^{0.6}}{{M_s}^{0.33}}\right) * 2 * R * S * k_h$$

$$M = \left(\frac{I * (R + 60)^4}{2975 * {M_s}^{0.1}} + 80\right) * k_h$$

Compared to the FEA models, the thrust equation is on average 1% conservative, maximum 34% conservative, and maximum 10% unconservative. The moment equation is on average 18% conservative, maximum 47% conservative, and maximum 5% unconservative.

Figure 8 shows the ratio of equation demand to FEA demand for thrust and moment, using the same method described for Figure 7.

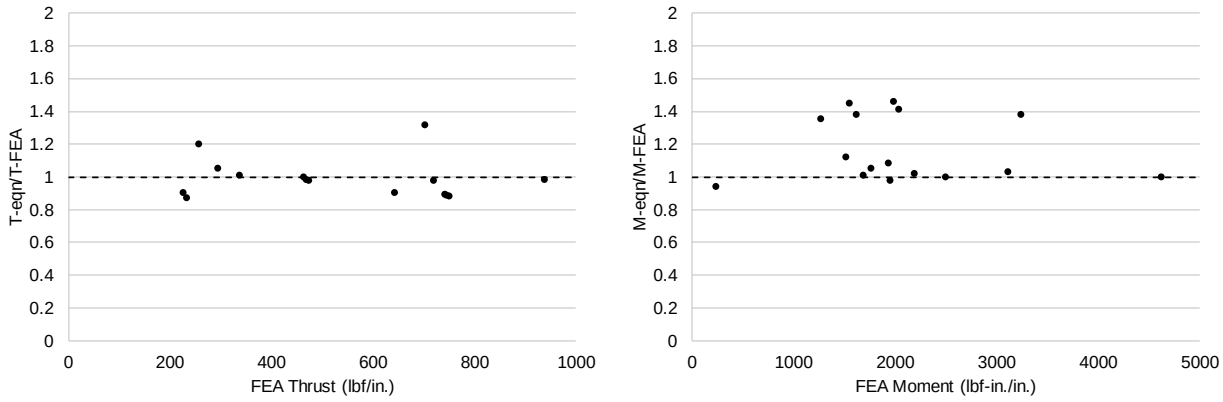

Figure 8 – Comparison of Equation and FEA Seismic Demands

Figure 9 further validates the equations by expanding the demand comparison for additional FEA models not used in the development of the equations. The equations are overly conservative for very good native soils (Ms = 5-6 ksi) but are reasonably conservative for more typical native soils (Ms = 0.5-3 ksi). The results labeled "Aluminum" are from an analysis considering a 9 in. by 2 in. aluminum box culvert with a 40 ft span, 10 ft rise, and 5 ft fill depth and show that the equations are appropriately conservative. This is as expected since the lower modulus of elasticity for aluminum compared to steel will result in less stress in the bridge for similar levels of deflection. The results labeled "ML95" are from an analysis similar to Model 1 but with an embedment soil material stiffness of E = 3,000 psi and demonstrate that the equations are reasonably conservative for ML embedment soils with 95% compaction or greater and SW embedment soils with 85% compaction or greater.

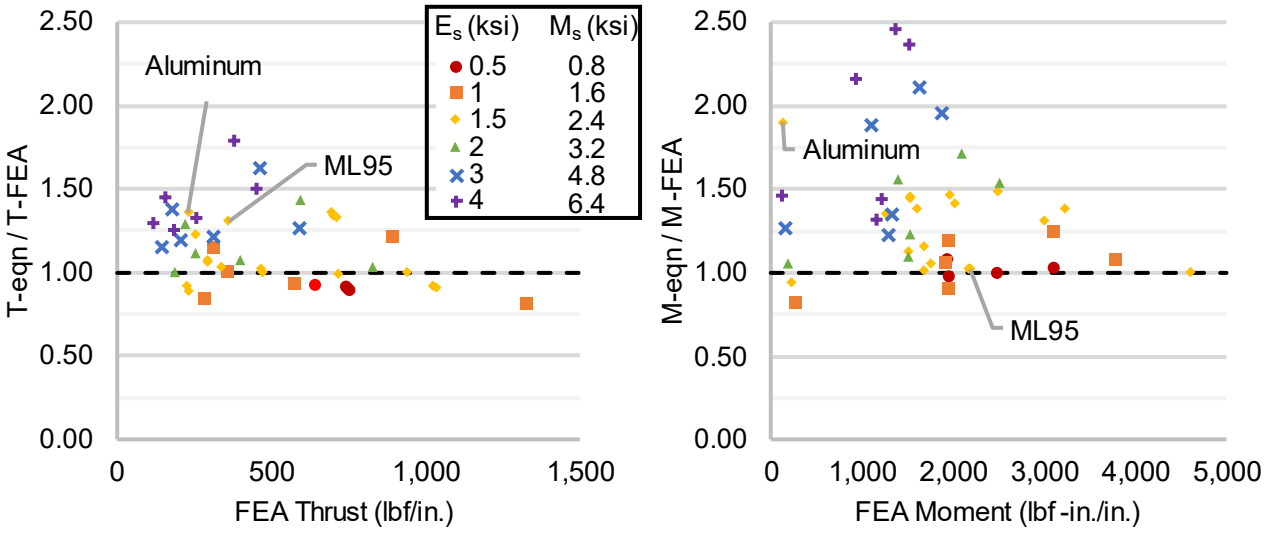

Figure 9 – Expanded Comparison of Equation and FEA Seismic Demands

The seismic thrust and moment equations are deemed applicable to the range of installations shown in Table 1 and additionally provide reasonable conservative results for aluminum structures and embedment soils within the stiffness range of E = 3,000 psi to 10,000 psi. They estimate only seismic demands and should be combined with existing approaches to calculate dead and live loads using Extreme Event load combinations from AASHTO Section 3. Appendix B shows a sample application of the equations.

3.4.1 Selection of Native Soil Stiffness

Native soil stiffness was included in both equations with exponent calibration factors to capture the non-linear effect. While the shear modulus (G) is most directly applicable to the seismic behavior of the native soil and the elastic modulus (E) is the required input for the FEA models on which the equations are based, we chose the constrained modulus (M_s) to represent the native soil stiffness as it can be readily estimated from existing design guidance or easily determined in soils testing, allowing for more practical use of the equations.

AASHTO Table 12.12.3.5-1 provides guidance on constrained modulus values based on soil type, compaction condition, and overburden pressure. These values are intended for embedment material rather than native material.

AWWA M45 provides guidance on conservative constrained modulus values for native soils based on soil type and geotechnical findings. These recommendations are shown in Table 4. For granular soils, values are based on blow count, N, at the buried structure elevation in accordance with ASTM D1586. For cohesive soils, values are based on unconfined compressive strength, q_u, in accordance with ASTM D2166.

Table 4 – Constrained Modulus of Native Soils

Granular Soils		Cohesive Soils		Constrained Modulus, M_{sn} (psi)
Blow Count, N (blows/ft)	**Description**	**Unconfined Compression Strength, q_u (psi)**	**Description**	
0 to 1	Very, very loose	0 to 0.4	Very, very soft	50
1 to 2	Very loose	0.4 to 0.9	Very soft	200
2 to 4	Loose	0.9 to 1.7	Soft	700
4 to 8	Loose	1.7 to 3.5	Medium	1,500
8 to 15	Slightly compact	3.5 to 7.0	Stiff	3,000
15 to 30	Compact	7.0 to 14.0	Very stiff	5,000
30 to 50	Dense	14.0 to 21.0	Hard	10,000
> 50	Very dense	> 21.0	Very hard	20,000

Note that constrained modulus values for very loose / very soft native soils and worse are outside the range of parameters considered when developing the seismic design equations. Installations with these conditions still require finite element modeling to determine seismic demands.

3.4.2 Selection of Lateral Acceleration Coefficient

The seismic lateral acceleration coefficient captures the magnitude of the earthquake event. AASHTO Section 3.10.2 specifies the peak ground acceleration (PGA) by geographical location. AASHTO Section 3.10.3 modifies the PGA based on the local soil conditions (site class) to give a base lateral acceleration coefficient.

AASHTO Section 11.6.5.2.2 allows for reduction of the base lateral acceleration coefficient to account for flexibility of buried walls. As detailed in NCHRP 611, relatively flexible walls that can tolerate several inches of lateral deformation can be designed for reduced seismic demand, typically taken as 50% of the base lateral acceleration coefficient. The NCHRP 611 findings are

specific to walls and have not been validated for corrugated arch-shaped metal structures. Further research should be conducted to examine whether a reduced seismic demand is appropriate for design of corrugated metal buried structures, which are traditionally considered flexible.

The design example shown in Appendix B applies the 50% reduction in seismic demand from AASHTO Section 11.6.5.2.2. An alternative approach would be to apply the full seismic demand, allow flexural yielding (plastic hinge formation) in the structure in an earthquake, and ensure that the soil support around the structure is sufficient to maintain static stability for axial load. This matches the approach used for design of typical shallow-corrugated metal buried structures (pipes), where moment is not considered in design as the soil envelope is judged to provide static stability.

3.5 Compare to AASHTO Strength I Load Combination

In order to determine the effect of the seismic demand equations on design of typical buried corrugated metal structures, Figure 10 compares total thrust from the controlling AASHTO seismic load combination (Extreme Event I) to total thrust from the controlling AASHTO dead and live load combination (Strength I). Note that this comparison is not shown for moment demand, as dead and live load moment calculation for deep-corrugated structures would require additional FEA modeling per AASHTO Section 12.8.9.3.2.

Four combinations of fill depth, native soil stiffness, and PGA are considered. Each point in each plot represents one design. The horizontal axis denotes the span of the structure, and the point type (e.g. circle, square, etc.) denotes the structure shape. The vertical axis is the ratio of Extreme Event I thrust demand to Strength I thrust demand. A ratio greater than 1.0 indicates that seismic demands control the design of the structure.

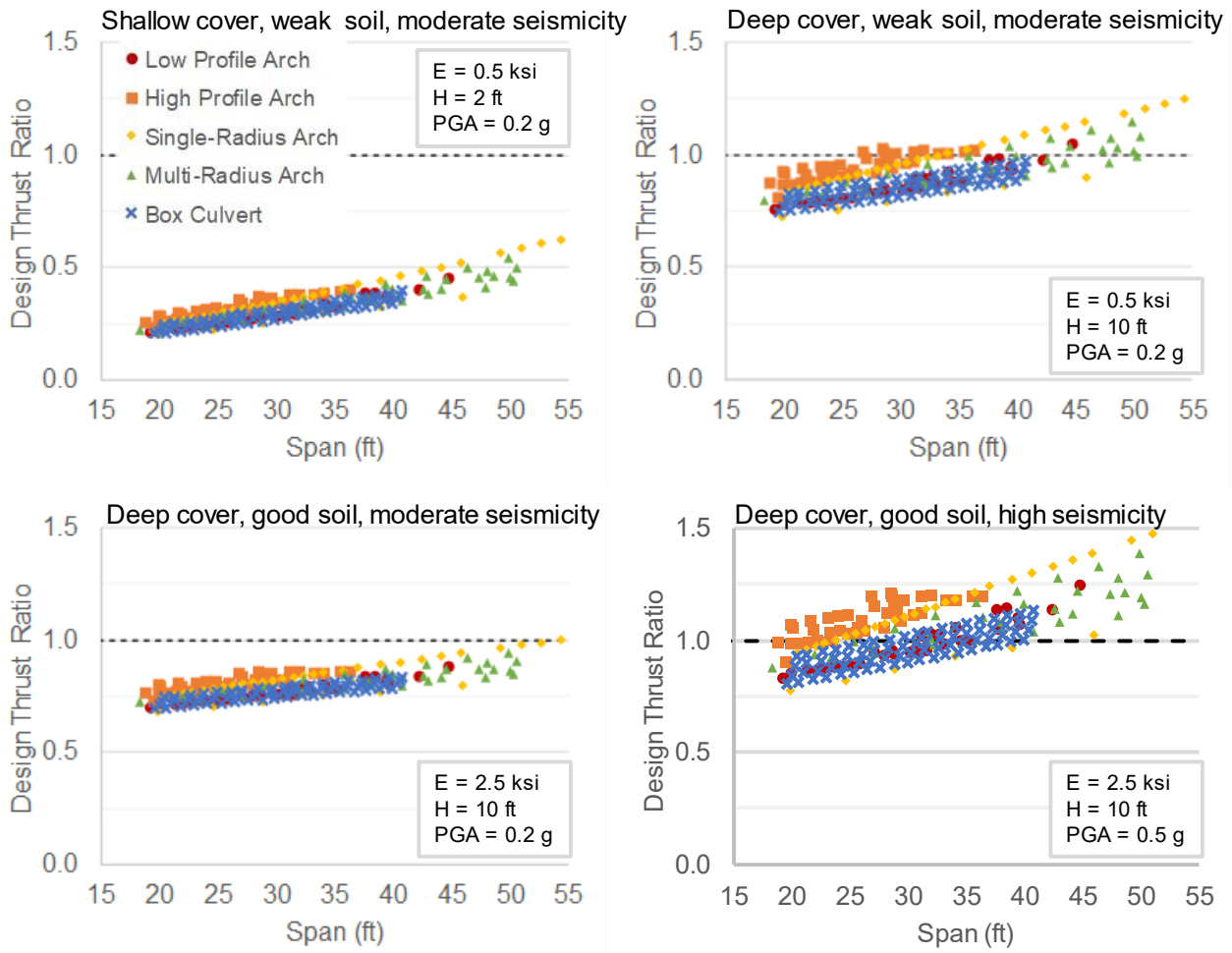

All runs: 7 GA 15x5.5, 120 pcf soil, E = native soil elastic modulus, H = fill depth, PGA = peak ground acceleration

Figure 10 – Effect of Seismic Demands on Design
(Design Thrust Ratio = Extreme Event I (Seismic) Thrust / Strength I (DL+LL) Thrust)

The design thrust ratio increases as the span increases, indicating that seismic demands are more sensitive to span than dead load demands are. Similarly, the ratio increases with increasing rise, as demonstrated by higher design thrust ratios for high-profile arches as compared to low-profile arches and box culverts of similar spans.

Seismic demands control only for structures with large span, deep fill, poor native soil, or high seismicity. This aligns well with field experience described previously, that buried structures typically perform well in seismic events. We recommend further research to evaluate the effects of service deterioration.

4. CONCLUSIONS

The thrust and moment equations shown in Section 3.4 provide a conservative estimate of seismic thrust and moment demand for the range of corrugated metal buried arch-shaped structures defined in Table 1 as compared to finite element analysis results. The equations were developed using methods consistent with existing AASHTO design approaches and can be readily used by designers as a screening tool to determine whether seismic demands are of concern for a given installation.

Installations with larger structure span, deep cover, poor native soil, or high site seismicity are most likely to be controlled by seismic demand. The design equations may be overly conservative for installations in very good native soils, but seismic demands are unlikely to control the design in these cases based on AASHTO load combinations. The design equations do not consider locations with faults, liquefaction, low-quality backfill, deep foundations, structure slopes, or surface ground slopes, which should be evaluated using SSI FEA based on the specific site conditions.

Appendix C details recommended modifications to AASHTO LRFD to implement the seismic design equations for corrugated metal buried arch-shaped structures.

5. RECOMMENDATIONS

The following are recommendations for additional research to extend the range of applicability of the new equations.

- Extend comparison of pseudo-static acceleration and static racking approaches for modeling seismic demands in order to address variable preferences among researchers and reviewers.
- Investigate whether the Newmark reduction in lateral seismic acceleration detailed in NCHRP 611 for buried walls is appropriate for corrugated metal buried structures.
- Determine whether deep-corrugated buried structures can reliably retain static stability after plastic hinge formation, allowing design for flexural yielding under seismic loading.
- Evaluate variations in structural backfill width.
- Evaluate variations in backfill materials to include recycled backfill.
- Evaluate the effects of service deterioration (e.g. corrosion) on seismic demand.
- Obtain field measurements of recently installed larger span structures (within the past fifteen years) that have been subjected to seismic loading and document performance, including comparisons with the proposed methodology.

6. REFERENCES

1. Earthquake Engineering Research Institute (EERI). *Loma Prieta Earthquake Reconnaissance Report*, 1990.
2. Hashash, Y., et al., *Seismic Design and Analysis of Underground Structures*, Tunneling and Underground Space Technology, 2001.
3. Isenberg, J. *The Role of Corrosion in the Seismic Performance of Buried Steel Pipelines*. NSF RA-780226, June 1978.
4. Youd, T.L. and Beckman, C.J. *Highway Culvert Performance During Past Earthquakes*, NCEER-96-0015, Nov. 1996.
5. American Association of State Highway and Transportation Officials, *AASHTO LRFD Bridge Design Specifications*.
6. Davis, C.A. and Bardet, J.P. *Responses of Buried Corrugated Metal Pipes to Earthquakes*, Journal of Geotechnical and Geoenvironmental Engineering, Jan. 2000.
7. Nakamura, S., Yoshida, N., Iwatate, T. *Damage to Daikai Subway Station During the 1995 Hyogoken-Nambu Earthquake and Its Investigation*. Japan Society of Civil Engineers, Committee of Earthquake Engineering, 1996.
8. EQE International. *Kobe Earthquake Summary Report*, 1995.
9. *Reinforced Concrete Box Structures*. Caltrans Memo to Designers 23-1, June 2017.
10. Khaleghi, B. *Buried Structures Design Memorandum*. Washington State Department of Transportation, 30 June 2014.
11. FHWA-NHI-10-034. *Technical Manual for Design and Construction of Road Tunnels – Civil Elements*. US Department of Transportation Federal Highway Administration, December 2009.
12. Al Atik, L., N. Sitar, *Development of Improved Procedures for Seismic Design of Buried and Partially Buried Structures*, Pacific Earthquake Engineering Research Center, 2007.
13. Wang, J.N. *Seismic Design of Tunnels – A Simple State-of-the-Art Design Approach*. Parsons Brinckerhoff Monograph 7, June 1993.
14. Tohda, J., et al., *Centrifuge Model Tests and Elastic FE analysis on Seismic Behavior of Buried Culverts*, Japanese Geotechnical Society, Asian Regional Conference on Soil Mechanics and Geotechnical Engineering, 2015.
15. Ulgen, D., et al., *Assessment of Racking Deformation of Rectangular Underground Structures by Centrifuge Tests*, Geotechnique Letters, Vol. 5, 261–268, 2015.
16. Anderson, D. et al. *Seismic Analysis and Design of Retaining Walls, Buried Structures, Slopes, and Embankments*. NCHRP Report 611, 2008.
17. McGrath, T.J., *Structural Investigation of Metal Box Sections with Spans up to 36 ft*
18. Moore, I.D., *Elastic Buckling of Buried Flexible Tubes – A Review of Theory and Experiment*. Journal of Geotechnical Engineering, 1989.

19. McGrath, T. J., *Calculating Loads on Buried Culverts*, Transportation Research Record 1656 Paper No. 99-0909, January 1999.

20. Katona, M.G. *Seismic Design and Analysis of Buried Culverts and Structures*. ASCE Journal of Pipeline Systems Engineering and Practice, Aug 2010.

21. Bowers, J.T., M.C. Webb, and J.L. Beaver, Soil Parameters for Design with the 3D Plaxis Hardening Soil Model, Transportation Research Record, June 2019.

22. Keene, R.W and J.L. Beaver, *Optimization as Applied to Design of Thermoplastic Pipe Profiles*, Proceedings of the Transportation Research Board Conference 2018, Washington, D.C., January 2018.

Appendix A

Literature Review

TABLE OF CONTENTS

A1. SEISMIC PERFORMANCE OF BURIED CORRUGATED METAL STRUCTURES

A1.1 Background

Buried structures have generally performed well in seismic events. Structures subject to ground failure such as fault rupture or liquefaction have failed, but structures subject only to ground motion have shown much less damage than nearby above-ground structures. However, some isolated cases of failure of buried structures in earthquakes have been reported.

The following sections detail the observed performance of buried structures in recent large seismic events. The seismic events range in magnitude and location, and the affected structures range in material, fill depth, and consideration of seismic loading in design. Our literature review did not identify detailed performance data for buried structures under seismic load (e.g., seismic deflections or strain measurements), but the general observed performance is valuable when considering theoretical behavior as described in Section A3.

A1.2 Recent Large Seismic Events

A1.2.1 Loma Prieta Earthquake, 1989, CA, USA, Magnitude 6.9

The Alameda Tunnel, a 14 ft diameter precast concrete tube immersed in fill running from Oakland to Alameda Island, experienced minor structural cracking, and limited water leakage. This tunnel was originally built in 1927, with no consideration of seismic loading. Nearby measured peak horizontal ground accelerations (PGA) ranged between 0.1 and 0.25 g, lower than the design-level earthquake which is on the order of 1 g (*9,13*).

The Bay Area Rapid Transit (BART) subway system sustained no damage and was fully operational immediately after the earthquake. BART buried structures, primarily reinforced concrete tunnels in fill and soft clay under relatively shallow cover, were designed in the 1960s with consideration of seismic loading, including special seismic joints to allow differential movement between connected components (*13,20*).

Above-ground bridges and water pipelines sustained significant damage to the point of being inoperable.

A1.2.2 Northridge Earthquake, 1994, CA, USA, Magnitude 6.7

The Los Angeles Metro subway was partially built at the time and sustained no damage. The reinforced concrete tunnels, bored under up to 60 ft soil depth, remained intact, but water pipelines in the city were damaged. Nearby measured peak horizontal ground accelerations (PGA) ranged between 0.1 and 0.25 g, lower than the design-level earthquake (*10*).

Davis and Bardet inspected over sixty corrugated metal buried structures near the fault rupture with fill depths ranging from 2 ft to 40 ft in alluvium material (sand, silt, clay mixture) (*8*). About half of these structures were small and circular, with diameter less than 3.5 ft, and did not show any signs of damage due to the earthquake. The remaining larger structures were a mix of circular, elliptical, and arch shapes, with spans up to 13 ft. No signs of damage due to the earthquake were present in 90% of the larger structures. Three structures showed signs of residual lateral displacement but were still operational. One structure, an 8 ft diameter circular pipe at the San Fernando Dam, collapsed, likely due to higher local ground motion. There was no clear relationship between pipe shape or fill depth and seismic performance.

Contech Engineered Solutions (Contech) inspected sixteen corrugated metal buried structures with standard installation conditions, spans ranging from 20 to 40 ft, and shallow fill depths (less than 5 ft). All the structures were located within 30 mi. of the Northridge epicenter and were likely subject to peak ground accelerations on the order of 1 g. None of the structures showed signs of significant damage due to the earthquake (*6*).

A1.2.3 Hyogoken-Nambu Earthquake, 1995, Japan

The Dakai subway station in Kobe, a concrete box tunnel designed in 1962 without consideration of seismic loading, collapsed due to lateral racking of the top slab causing failure of the supporting columns. Less damage occurred near the ends of the tunnel, where the end treatments acted as shear walls to resist deformation (*19*). Collapse investigation noted that the construction method used prevented compaction of the backfill material adjacent to the structure, removing soil support and causing the tunnel to act more similarly to an above-ground structure (*11*).

A1.2.4 Other

Isenberg examined damaged steel pipes from the 1965 Puget Sound, 1969 Santa Rosa, and 1971 San Fernando earthquakes, finding that all damage occurred at locations where existing corrosion had reduced the capacity of the pipe (*15*). Subsequent design calculations based on recorded ground motions, and observation of adjacent sections with no corrosion, showed that the pipes could have withstood the seismic demands had they not been corroded.

Youd and Beckman inspected and reviewed performance of seventeen corrugated metal pipes subject to the 1964 Alaska, 1971 San Fernando, 1983 Borah Peak, 1989 Loma Prieta, 1993 Hokkaido Nansi-Oki, and 1994 Northridge earthquakes, focusing on structures with reported damage (*26*). They found that all major damage and failures were due to ground failure, including liquefaction, slope instability, and fault rupture. They found no other damage to the structures due to seismic motion.

A2. CURRENT SEISMIC DESIGN OF BURIED STRUCTURES

A2.1 Code Requirements

Current structural design codes do not calculate lateral seismic demands on typical buried structures. This has historically been justified by the relatively small amount of damage observed in buried structures in previous earthquakes, as discussed in Section A1.

AASHTO LRFD Bridge Design Specifications (AASHTO) Section 12.6.1 specifies that "earthquake loads should be considered only where buried structures cross active faults" (*2*). This condition is not common. Section 3.10.1, which defines seismic hazards for typical above-ground bridge structures, states that "seismic effects for box culverts and buried structures need not be considered, except where they cross active faults."

Canadian Highway Bridge Design Code (CHBDC) Section 7.5.8 specifies that "buried structures shall be designed to resist inertial forces associated with a seismic event having a 2% chance of being exceeded in 50 years." No method for calculating the "inertial forces" is provided. CHBDC also specifies that vertical earthquake demands be considered by amplifying the dead load demand by two-thirds the peak horizontal ground acceleration (*7*).

Both AASHTO and CHBDC specify methods for calculating dynamic earth pressures. These are intended for use in designing retaining walls and are based on the Mononobe-Okabe method. As discussed in Section A3.2.3, these methods are not appropriate for use in calculating seismic demands on buried structures.

AASHTO and CHBDC both modify seismic demands based on importance category, specifying lower forces for unoccupied structures.

A2.2 State DOT Policies

US state-level departments of transportation (DOTs) generally do not address seismic design of buried structures beyond referring to AASHTO specifications. Exceptions are Washington and California, two of the most seismically active states.

Washington State DOT (WSDOT) published a design memorandum on buried structures in 2014 requiring consideration of seismic demands for buried structures with spans greater than 20 ft (*18*). WSDOT states that both unstable ground conditions (e.g., fault effects, liquefaction) and lateral racking deformations should be considered. WSDOT refers to FHWA-NHI-10-034 for seismic design, which recommends the methods discussed in Sections 3.2.4.2 and 3.2.4.3 (*12*).

California DOT (Caltrans) published a memorandum to designers in 2017 (*5*) requiring consideration of seismic demands for buried reinforced box culverts with spans greater than 20 ft. Caltrans mentions lateral racking deformations and fault effects but does not provide a method for seismic design.

A3. IMPROVED SEISMIC DESIGN OF BURIED CORRUGATED METAL STRUCTURES

Based on the historical performance of buried structures and the current code approaches, seismic demands should not often control design of buried structures. However, buried structures are being installed for an expanding variety of applications and locations, with increasing dimensions (rise and span). A growing number of buried structures are located where seismic demands may be significant, or where the consequence of failure requires that seismic load cases be considered in design. Developing a simple and conservative seismic design methodology will identify installations where seismic performance may not be adequate. Widespread seismic design of buried structures will also aid probabilistic risk assessment of larger transportation systems.

A3.1 Deformation and Behavior

Seismic effects on buried structures are fundamentally different than seismic effects on traditional, above-ground structures. In an earthquake, ground motion shakes the base of above-ground structures. The structure has inertia (resistance to motion) due to its weight, so the motion of the structure lags behind the motion of the ground, as shown in Figure 1a. The resulting differential displacement within the structure generates structural force demands, which are primarily a function of the earthquake magnitude and characteristics, the weight of the structure, and the stiffness of the structure. Code-based seismic design approaches for above-ground structures (e.g., IBC, AASHTO, ASCE) estimate seismic forces based on these concepts.

Buried structures are surrounded by soil, so earthquake ground motions are applied to the full height of the structure rather than just the base. This typically prevents any significant inertial effects but applies soil pressures and displacements over the height of the structure, as shown in Figure 1b.

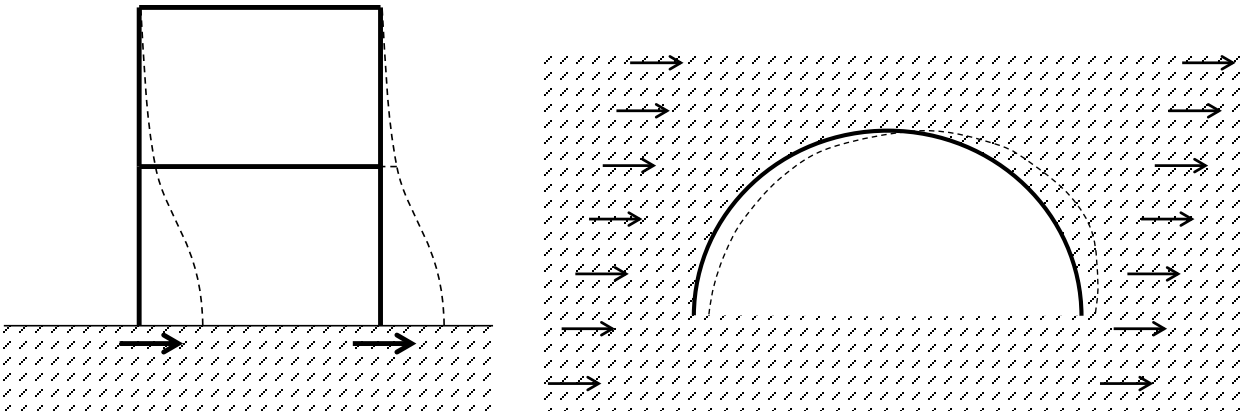

Figure 1 – Effect of Horizontal Seismic Ground Motion on (a) Above-Ground Structures (Buildings) and (b) Buried Structures (Culverts and Buried Bridges)

Buried structures are subject to horizontal and vertical ground motions in three dimensions. The impact of these ground motions can be broken into vertical, longitudinal, and lateral effects, as shown in Figure 2. Buried structures may also be subject to ground failures.

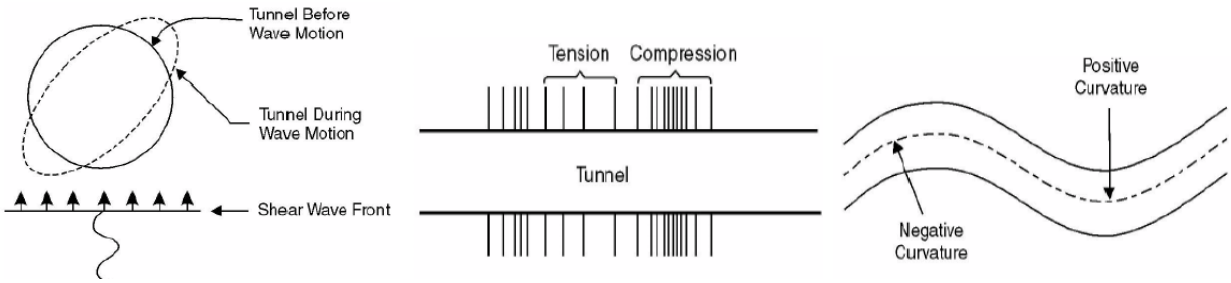

Figure 2 – Response of Buried Structures to Directional Ground Motions (Modified from 12)

A3.1.1 Vertical Ground Motion

Vertical ground motions are generally less severe than horizontal ground motions, with vertical peak ground acceleration (PGA) often assumed to be two-thirds horizontal PGA (*12*). Vertical ground motion amplifies the vertical loads on a buried structure, causing the same deformation behavior of the structure as dead load. The vertical seismic effect can be accounted for by increasing the dead load factor in seismic load combinations by the vertical PGA. Seismic load combinations generally have reduced dead load factors and live load magnitudes, reflecting the reduced probability that the maximum design load would occur simultaneously with a seismic

event, so vertical seismic effects generally do not control for buried structures with relatively shallow fill depth.

A3.1.2 Longitudinal Ground Motion

Longitudinal effects of horizontal ground motion can occur along the length of long, linear structures. Friction between the structure and soil can develop longitudinal axial force (tension or compression) in the structure. Differential lateral displacement along the length (e.g., due to differing ground conditions) can cause longitudinal bending of the structure. These deformation behaviors occur in long pipelines but are unlikely to develop in relatively short structures such as culverts (*3*). The relatively limited length does not provide sufficient soil contact to develop significant axial force. The limited length and standardized installation conditions make differential lateral displacements along the length unlikely.

In addition, corrugated metal structures have significant longitudinal flexibility due to folding of corrugations (similar to an accordion). They are therefore designed as two-dimensional (2D) sections with no consideration of longitudinal effects. Any longitudinal bending or axial deformations that may occur in corrugated metal structures in an earthquake should be easily tolerated without development of significant longitudinal force. This is consistent with observed field performance.

A3.1.3 Lateral Ground Motion

Lateral effects of horizontal ground motion cause racking of buried structures, referred to as ovaling for round pipes. This is the primary form of seismic loading applicable to short-length, low-longitudinal-stiffness buried structures such as corrugated steel culverts (*12*). The magnitude of racking is a function of the earthquake magnitude, soil properties, fill depth, structure geometry and stiffness, and soil-structure interaction.

3.1.3.1 Free-Field Deformation

Free-field deformation refers to the lateral (shear) deformation of the ground alone, away from any buried structures, due to seismic ground motion. The free-field deformation of the ground in an earthquake is traditionally calculated using wave propagation theory, which is appropriate

for very deep fill depths (*24*). Culverts are typically installed with shallow fill depths (less than 20 ft), where the free-field deformation is better estimated as a function of the PGA, fill depth, and soil shear modulus as described in Section 3.2.4.1.

3.1.3.2 Soil-Structure Interaction

Introducing a buried structure changes the seismic deformation of the soil. If the structure has lateral stiffness greater than the surrounding soil, the racking deformation will be less than free-field deformation as the structure reinforces the soil. If the structure is less stiff than the surrounding soil, the racking deformation may be greater than the free-field deformation as the structure effectively acts as a hole in the soil. Existing methods for determining the effects of soil-structure interaction on deformation are discussed in Section A3.2.4.

A3.1.4 Ground Failure

Ground failure can occur in many forms, including fault rupture, liquefaction, or landslides. All these conditions remove critical support from buried structures. It is generally not feasible to design buried structures to withstand ground failure (*24*). Instead, designs should ensure measures to mitigate risk to structures, including competent ground around the structure through selection of appropriate backfill materials, improvement or removal of unsuitable native soils, and avoidance of known fault locations.

A3.2 Existing Approaches

Existing approaches for seismic design of buried structures either perform physical testing, run detailed seismic soil-structure interaction (SSI) finite element analysis (FEA), estimate dynamic lateral soil pressures on the structure, or estimate lateral racking deformation of the structure (3,13). The advantages and disadvantages of each of these approaches are discussed in the following sections.

A3.2.1 Physical Testing

Centrifuge testing has frequently been used in past research to directly apply ground motion to small-scale models of buried structures (*1,13,22,23*). A scale model of the buried structure and surrounding soil is placed at one end of a centrifuge arm. As the arm spins, the structure model

is rotated so that the lateral direction of the structure model is in the global vertical direction and the vertical direction of the model is parallel to the axis of the centrifuge arm. The rotation of the arm is set to impose the desired vertical confining pressure on the soil in the model. Global vertical shaking is then applied to the arm to simulate lateral ground motion in the model. This setup is shown schematically in Figure 3.

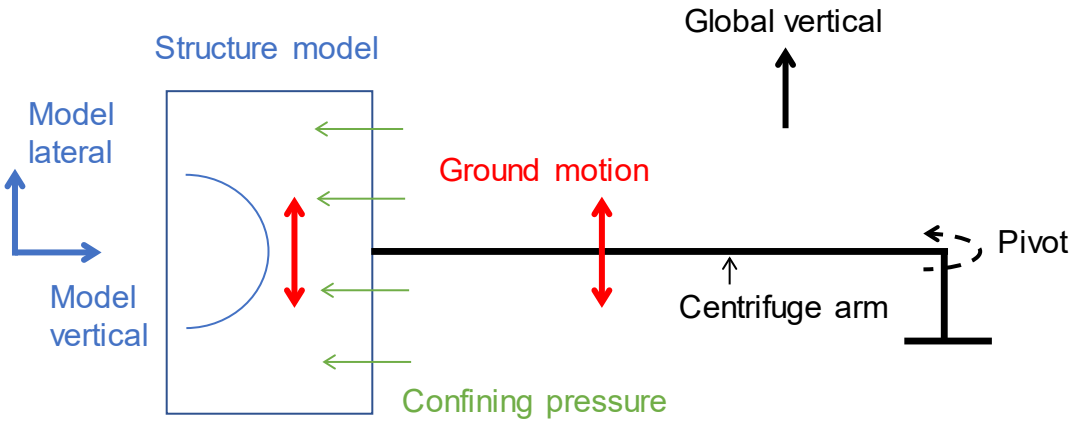

Figure 3 – Setup for Centrifuge Physical Testing

Centrifuge testing allows realistic simulation of soil stress at depth with small-scale models and application of widely varying ground motions for repeatable and relatively cost-effective physical testing. It requires complex scaling of dimensions and results but is effective for research studies on behavior (*1*) and physical validation of theoretical and numerical behavior predictions.

Centrifuge testing is not practical for design. Comparison of centrifuge test results to results of SSI FEA using lateral racking deformations (similar to the approach described in Section A3.2.4 below) has shown that SSI FEA can accurately model lateral ground motions and can be used in place of parametric physical testing (*22*).

A3.2.2 SSI FEA

Detailed SSI FEA is the most accurate analytical method to determine the deformation of a buried structure under selected seismic load. A finite element model (FEM) of the structure and surrounding soil is generated in 2D or 3D depending on the installation conditions. Ground

deformations are then applied to the model, and the resulting deformations and internal forces (demands) in the structure are determined for design (*17*).

The ground motions can be applied dynamically or quasistatically. The dynamic approach is more refined but requires detailed knowledge of soil dynamic properties (e.g., shear wave velocity, peak particle velocity) that are not easily determined by physical testing. The quasistatic approach applies seismic demands as enforced displacements without inertial effects, which is appropriate for typical culvert fill depths (less than 20 ft), as described in Section 3.2.4.1. The static deformations calculated using this approach should be applied at both vertical boundaries of the FEM, as well as the top boundary (ground surface). Research has shown that results from the static approach match well with physical testing and theoretical solutions (*4,17,22*).

The SSI FEA approach is applicable to a wide range of structure geometries and materials, as well as all backfill materials and cover heights. It also provides the ability to model partial slip conditions between the buried structure and surrounding soil. However, SSI FEA may not be practical for all buried structure installations due to the time and cost associated with modeling.

A3.2.3 Dynamic Soil Pressures

Dynamic soil pressure methods calculate seismic lateral earth pressures due to soil inertial effects. Buried structures could theoretically be designed to resist these additional lateral pressures.

The Mononobe-Okabe (MO) method for determining dynamic soil pressures has been adopted by AASHTO, CHBDC, and Japanese Code (*16*). The MO method was developed specifically for above-ground retaining walls and assumes that a soil failure plane can form behind the wall (*21*).

For buried structures, the MO method would be most appropriate for concrete box culverts at shallow fill depths, which have similar geometry and flexibility to above-ground retaining walls. However, as discussed in Section A3.1, corrugated steel buried structures move together with

the soil making development of a soil failure plane at depth unlikely. Comparison of physical testing to MO predictions for concrete buried structures has shown that the MO method is over-conservative, to the point of being physically unrealistic (*1,24*). Other dynamic pressure methods, such as the Wood method, have shown similar results (*25*).

Available dynamic pressure methods are not appropriate for use with buried corrugated steel structures, as the structures do not match the geometry or stiffness assumed in the development of the methods.

A3.2.4 Lateral Racking Deformations

Lateral ground displacement can be calculated independent of the structure as the free-field deformation shear strain with depth as described in Section 3.1.3.1. Estimates of soil-structure interaction can then be used to modify the free-field deformation and apply it directly to the structure. For simple circular structures, closed-form solutions are available. For rectangular structures, methodologies have been developed based on simple structural analysis models. No closed-form methods have been developed for arch-shaped structures, such as the typical corrugated steel buried structure shapes shown in Figure 4.

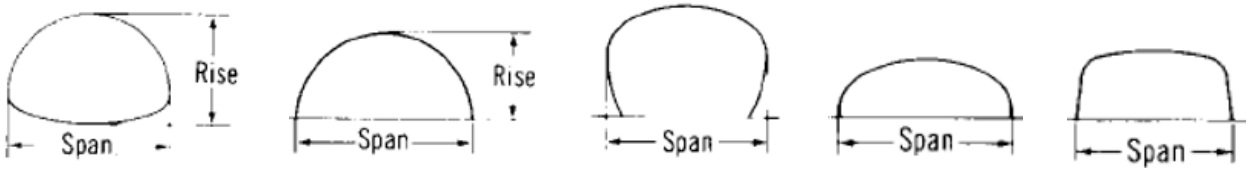

Figure 4 – Typical Arched Buried Corrugated Steel Structure Shapes

3.2.4.1 Free-Field Deformation

Lateral free-field deformations can be calculated as follows (*3*):

$$\gamma_{max} = \frac{\tau_{max}}{G} = \frac{PGA * \sigma_v * R_d}{G}$$

γ_{max} = maximum free-field shear strain

τ_{max} = maximum seismic shear stress

PGA = peak ground acceleration (g)

σ_v = overburden stress at base of culvert (unit weight of soil times depth)

G = effective strain-compatible shear modulus of soil surrounding culvert

R_d = factor to reduce PGA (specified at surface) based on fill depth

$R_d = 1 - 0.00233z$ for z < 30 ft (typical for culverts)

$R_d = 1.174 - 0.00814z$ for 30 ft < z < 75 ft

z = depth from surface to base of culvert (ft)

Free-field deformations can also be calculated using the shear-wave peak particle velocity for the soil (not often available) or using a seismic response analysis computer program such as SHAKE. Use of such programs is required when multiple distinct soil layers occur over the heights of the buried structure.

The diameter change resulting from ovaling of a circular buried structure corresponding to the free-field deformation can be calculated assuming a constant soil body (free-field shear), or assuming a zero-stiffness opening in the soil at the culvert.

$\Delta D_{ff} = 0.5 * \gamma_{max} * D$

$\Delta D_{so} = 2 * \gamma_{max} * (1 - v) * D$

ΔD_{ff} = culvert diameter change assuming constant soil body (free-field)

ΔD_{so} = culvert diameter change assuming opening at culvert location (soil opening)

D = culvert diameter

v = soil Poisson Ratio

For a typical backfill material Poisson Ratio of 0.3, the diameter change assuming an opening is almost three times greater than the diameter change assuming no opening. Rigid structures (e.g., concrete) are stiffer than typical surrounding soils and will experience less deformation than either estimate. Flexible structures (e.g., corrugated steel) are typically more flexible than the surrounding soil and will experience deformation between the two estimates, but often closer to ΔD_{so}. Consideration of the relative stiffness of the soil and the structure (soil-structure interaction) is required to improve the deformation estimate and ensure safe designs.

3.2.4.2 Closed-Form Solutions for Circular Structures

For circular buried structures, closed-form approaches have been developed to estimate the lateral racking deformation and resulting internal forces as a function of the structure stiffness, the soil material properties, and the level of slip between the soil and structure.

The structure axial and flexural stiffnesses are quantified by compressibility (C) and flexibility (F) ratios, respectively, calculated as follows (*3*).

$$C = \frac{E_m(1 - {v_l}^2)R}{E_l A_l(1 + v_m)(1 - 2v_m)}$$

$$F = \frac{E_m(1 - {v_l}^2)R^3}{6E_l I_l(1 + v_m)}$$

E_m = strain-compatible elastic modulus of soil (consistent with G)

E_l = elastic modulus of structure

A_l = cross-sectional area of structure (per unit length)

I_l = moment of inertia of structure (per unit length)

v_m = Poisson Ratio of soil

v_l = Poisson Ratio of structure

R = nominal radius of structure

Assuming full slip between the soil and structure, the maximum thrust (T) and moment (M) in the structure can be calculated as follows (*3*):

$$T = \frac{k_l E_m}{6(1 + v_m)} R\gamma_{max}$$

$$M = RT$$

$$k_l = \frac{12(1 - v_m)}{2F + 5 - 6v_m}$$

The full-slip thrust calculation is thought to significantly underestimate thrust in the structure, so calculating thrust using a no-slip assumption is recommended (*24*). The no-slip thrust calculation is more complex, so it is omitted here for clarity. No moment calculation is available for the no-slip assumption; however, the full-slip condition moment calculation has been shown to give conservative results.

3.2.4.3 Simplified Analysis Approach for Other Shapes

For rectangular concrete box culverts, the lateral deformation of the structure can be estimated using simplified structural analysis as follows (*3*):

$$\Delta_{ff} = H\gamma_{max}$$

$$\Delta_s = k_r \Delta_{ff}$$

$$k_r = \frac{2F_r}{1 + F_r}$$

$$F_r = \frac{GL}{K_s H}$$

L = span of structure

K_s = lateral stiffness of structure

H = height of structure

The lateral stiffness of the structure (K_s) is the ratio of lateral force to lateral displacement at the top of the structure, which can be determined using a simple structural model. The flexibility ratio (F_r), developed for rectangular structures, can then be calculated to provide an estimate of the relative stiffness of the structure and soil and modify the free-field deformation (Δ_{ff}). The calculated lateral deformation (racking) of the structure due to seismic ground motion (Δ_s) can be applied in the same simple structural model to calculate seismic forces and moments. Other researchers have proposed slightly different equations for the structure stiffness design curve equation (k_r) that include the soil Poisson Ratio (*12,24*). The different equations give similar results for typical installation conditions.

Figure 5 compares results from the simplified analysis method to results from SSI FEA, showing good agreement for rectangular concrete box culverts. The effectiveness of this method for other structure types, such as corrugated metal arches, has not been studied.

	Structural Configurations and Soil Properties
Case 1	10' x 10' Square Box, in Firm Ground (E_m = 3,000 psi, ν_m = 0.3)
Case 2	10' x 10' Square Box, in Very Stiff Ground (E_m = 7,500 psi, ν_m = 0.3)
Case 3	10' x 20' Rectangular Box, in Firm Ground (E_m = 3,000 psi, ν_m = 0.3)
Case 4	10' x 10' Square 3-Sided, in Very Stiff Ground (E_m = 7,500 psi, ν_m = 0.3)
Case 5	10' x 20' Rectangular 3-Sided, in Very Stiff Ground (E_m = 7,500 psi, ν_m = 0.3)

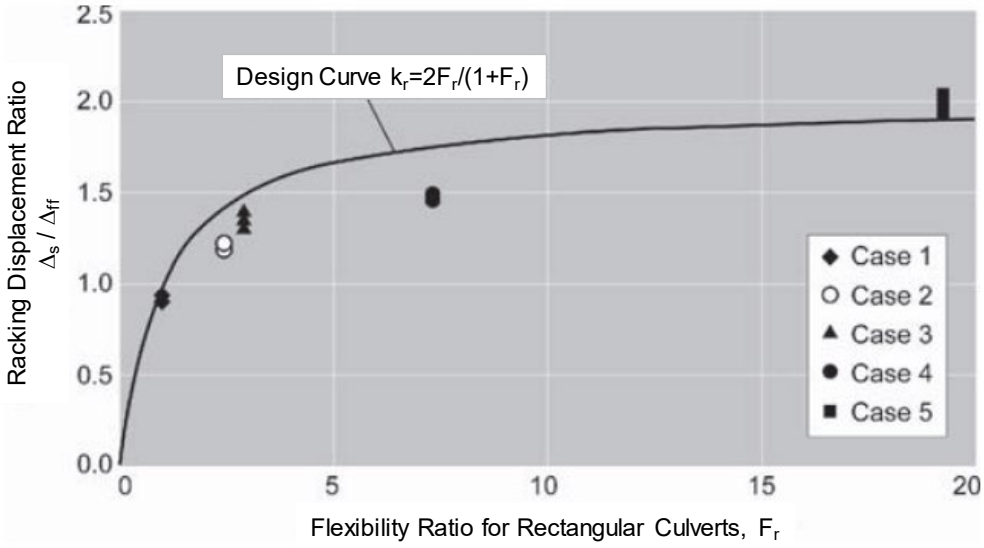

Figure 5 – Comparison of Lateral Racking from Simplified Analysis and SSI FEA (Modified from 3)

A3.3 Possible Improved Approaches for Corrugated Steel Buried Structures

Our preliminary comparison between SSI FEA, the closed-form equations for circular structures, and the simplified analysis approach for rectangular structures for seismic demands on a single corrugated steel arch, indicate that the simplified methods provide a reasonable, if slightly unconservative, estimate of moment, but do not accurately estimate thrust. The full-slip equation and simplified analysis approach significantly underpredict thrust, and the no-slip equation significantly overpredicts thrust.

Figure 6 shows the arch geometry (single radius regular arch) and SSI FEA model used for the comparison and plots thrust and moment demands from each approach. Thrust from the no-slip equation is excluded for clarity, as it is over six times larger than thrust from SSI FEA.

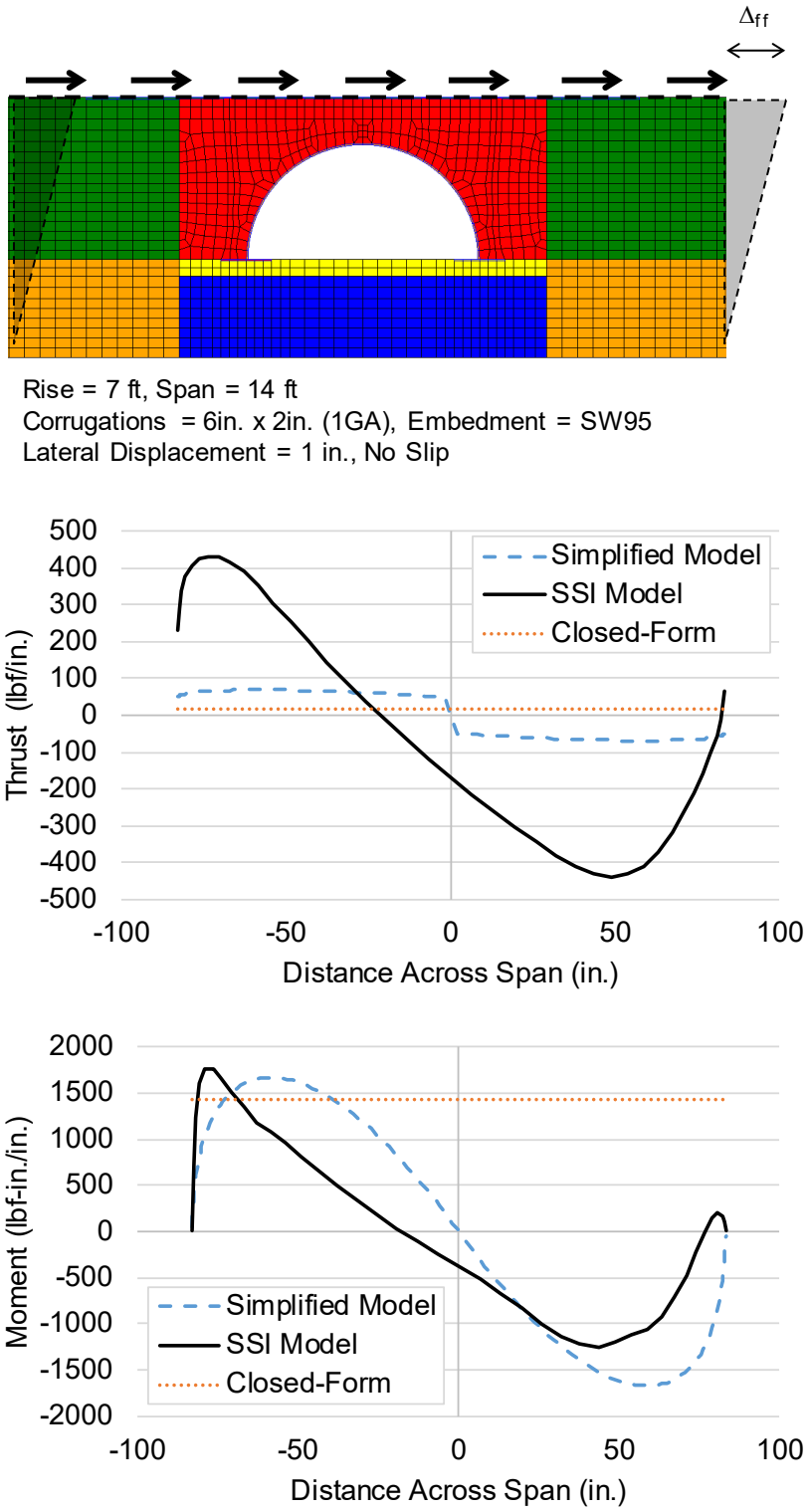

Figure 6 – Comparison of Seismic Demand Calculation Methodologies

A series of SSI FEA models should be run to confirm that these results hold for a wider range of installations. The SSI FEA models should include interface elements to evaluate conditions with

known friction behavior and should cover the typical range of the following installation parameters.

- Fill depth
- Span
- Rise
- Plate radius
- Overall geometry (e.g., single-radius arch, multiradius arch, pipe arch, box culvert)
- Corrugation size (e.g., 6 in. x 2 in., 15 in. x 5.5 in., 1 GA, 8 GA)
- Stiffeners (e.g., typical ribs for box culverts)
- Footing type (spread footing, closed-bottom, deep foundation)
- Structure material (e.g., steel, aluminum)
- Embedment material
- Native (in situ) materials and trench width
- Installation type (e.g., embankment, vertical trench, sloped trench)
- Earthquake magnitude

The additional SSI FEA can also provide a baseline for comparison for modifications to the existing simplified approaches. Modifications may include the following:

- Calibrate new structure stiffness design curve equation (k_r) for structure shapes and materials other than rectangular boxes.
- Addition of geometry correction factor to closed-form equations to account for deviation from circular shape. Analogous to R_h factor used in AASHTO global buckling calculations (Section 12.8.9.6) (*2*).

If the SSI FEA results reveal a clear pattern of behavior for seismic demands of buried corrugated metal structures, it may be more appropriate to develop a new, more suitable approach separate from the existing approaches. For example, the stiffness ratios (C, F) of large corrugated metal structures are typically high, at which point the structure stiffness design curve equations (k_r) converge towards constant values. This may allow use of a more simplified set of equations.

A4. CONCLUSIONS

Despite strong past performance of buried structures in earthquakes, some installations necessitate explicit design for seismic demands, which currently requires detailed finite element analysis. As larger-span buried bridge structures are more frequently built, these seismic analyses are more frequently required. Development of a simplified seismic design approach would allow efficient confirmation of structural adequacy under seismic demands for all installations. Existing approaches must be compared against detailed model results across a reasonably inclusive range of installation parameters to allow for appropriate modification of the existing approaches for use with corrugated metal buried structures.

A5. REFERENCES

1. Al Atik, L., N. Sitar, *Development of Improved Procedures for Seismic Design of Buried and Partially Buried Structures*, Pacific Earthquake Engineering Research Center, 2007.

2. American Association of State Highway and Transportation Officials, AASHTO LRFD Bridge Design Specifications, 8th Edition, 2017.

3. Anderson, D., et al., *Seismic Analysis and Design of Retaining Walls, Buried Structures, Slopes, and Embankments*, NCHRP Report 611, 2008.

4. Byrne, P.M., et al., Seismic Analysis of Large Buried Culvert Structures, Transportation Research Record 1541, 1996.

5. Caltrans, *Reinforced Concrete Box Structures*. Memo to Designers 23-1, June 2017.

6. Contech Engineered Solutions, *Contech Super-Span Performance within California Earthquake Zone*, 1995.

7. CSA Group, Canadian Highway Bridge Design Code, S6-19, 2019.

8. Davis, C.A. and Bardet, J.P. "Responses of Buried Corrugated Metal Pipes to Earthquakes," *Journal of Geotechnical and Geoenvironmental Engineering*, Jan. 2000.

9. Earthquake Engineering Research Institute (EERI), *Loma Prieta Earthquake Reconnaissance Report*, 1990.

10. Earthquake Engineering Research Institute (EERI), *Northridge Earthquake Reconnaissance Report*, 1995.

11. EQE International, *Kobe Earthquake Summary Report*, 1995.

12. FHWA-NHI-10-034, *Technical Manual for Design and Construction of Road Tunnels – Civil Elements*, US Department of Transportation Federal Highway Administration, Dec. 2009.

13. Hashash, Y., et al., *Seismic Design and Analysis of Underground Structures*, Tunneling and Underground Space Technology, 2001.

14. Hushmand, A., et al., "Seismic Performance of Underground Reservoir Structures: Insight from Centrifuge Modeling on the Influence of Structure Stiffness," *ASCE Journal of Geotechnical and Geoenvironmental Engineering*, 2016.

15. Isenberg, J., *The Role of Corrosion in the Seismic Performance of Buried Steel Pipelines*, NSF RA-780226, Jun. 1978.

16. Japanese Sewage Works Association (JSWAS), Earthquake Resistant Measures Guidelines and Commentary of Sewer Facilities, 2014, in Japanese.

17. Katona, M.G., "Seismic Design and Analysis of Buried Culverts and Structures*," ASCE Journal of Pipeline Systems Engineering and Practice*, Aug 2010.

18. Khaleghi, B., *Buried Structures Design Memorandum*, Washington State Department of Transportation, 30 Jun. 2014.

19. Nakamura, S., N. Yoshida, and T. Iwatate, *Damage to Daikai Subway Station During the 1995 Hyogoken-Nambu Earthquake and Its Investigation*, Japan Society of Civil Engineers, Committee of Earthquake Engineering, 1996.

20. Parsons, Brinckerhoff, Quage, and Douglas Inc., *Trans-Bay Tube Seismic Joints Post-Earthquake Evaluation,* report prepared for Bay Area Rapid Transit District, 1991.

21. Seed, B.H., and R.V. Whitman, *Design of Earth Retaining Structures for Dynamic Loads*. ASCE Specialty Conference on Lateral Stresses in the Ground and Design of Earth Retaining Structures, 1970.

22. Tohda, J., et al., *Centrifuge Model Tests and Elastic FE analysis on Seismic Behavior of Buried Culverts*, Japanese Geotechnical Society, Asian Regional Conference on Soil Mechanics and Geotechnical Engineering, 2015.

23. Ulgen, D., et al., "Assessment of Racking Deformation of Rectangular Underground Structures by Centrifuge Tests," *Geotechnique Letters*, Vol. 5, 261–268, 2015.

24. Wang, J.N., *Seismic Design of Tunnels – A Simple State-of-the-Art Design Approach*. Parsons Brinckerhoff Monograph 7, June 1993.

25. Wood, J.H., *Earthquake Induced Soil Pressures on Structures*, California Institute of Technology, Report No. EERL 73-05, 1973.

26. Youd, T.L., and C.J. Beckman, *Highway Culvert Performance During Past Earthquakes*, NCEER-96-0015, Nov. 1996.

Appendix B

Design Example

Introduction

This design example demonstrates how seismic demands calculated using the newly-developed seismic demand equations should be combined with traditionally-calculated dead and live load demands. The example uses a 6"x2" long-span high profile arch structure. The method of load combination is similar for deep corrugated structures and structural plate box structures, though the calculation of dead and live load demands would change. The base lateral acceleration coefficient is reduced by 50% to account for flexibility of buried walls; however, the applicability of this provision for corrugated arch-shaped metal structures has not been validated.

Installation Parameters

Span	$S := 30ft + 3in$	
Rise	$R := 15ft + 5in$	
Top arc radius	$R_T := 20ft + 7in$	
Fill depth	$H := 5ft$	
Soil unit weight	$\gamma_s := 120pcf$	
Profile	8 GA 6"x2"	
Area	$A_p := 2.449 \frac{in^2}{ft}$	
Yield strength	$f_y := 33ksi$	
Native soil constrained modulus	$M_s := 900psi$	AWWA M45 Table 5-6
Wheel load	$P_w := 16kip$	AASHTO 3.6.1.2.2
Tire patch length	$l_t := 10in$	AASHTO 3.6.1.2.5
Tire patch width	$w_t := 20in$	AASHTO 3.6.1.2.5
Live load distribution factor	$LLDF := 1.15$	AASHTO 3.6.1.2.6
Design horizontal peak ground acceleration	$PGA := 0.6$	AASHTO Figure 3.10.2.1-4
Zero-period site factor	$F_{pga} := 1.0$	AASHTO Table 3.10.3.2-1 Assuming Site Class D

Calculations

Peak seismic ground acceleration coefficient	$A_s := F_{pga} \cdot PGA = 0.6$		AASHTO Eq. 3.10.4.2-2
Base horizontal acceleration coefficient	$k_{h0} := A_s = 0.6$		AASHTO 11.6.5.2.1
Horizontal acceleration coefficient	$k_h := 0.5 k_{h0} = 0.3$		AASHTO 11.6.5.2.2 Note: this assumption should be verified on a structure-by-structure basis, aided by additional research
Dead load thrust	$T_{DL} := \frac{\gamma_s \cdot H \cdot (2 \cdot R_T)}{2}$	$T_{DL} = 12.35 \cdot \frac{kip}{ft}$	AASHTO 12.7.2.2-1
Live load patch length	$l_w := l_t + LLDF \cdot H$	$l_w = 6.58\,ft$	
Live load width	$C_L := \min(l_w, S)$	$C_L = 6.58\,ft$	AASHTO 12.7.2.2-2
Correction factor	$F_1 := \frac{0.54 \cdot \frac{S}{ft}}{\left(\frac{w_t}{12in}\right) + LLDF \cdot \frac{H}{ft} + 0.03 \cdot \frac{S}{ft}}$	$F_1 = 1.96$	AASHTO 12.7.2.2-5
Live load thrust	$T_{LL} := \frac{1}{2} \cdot \frac{P_w}{(l_t + LLDF \cdot H) \cdot (w_t + LLDF \cdot H)} \cdot C_L \cdot F_1$	$T_{LL} = 2.12 \cdot \frac{kip}{ft}$	AASHTO 12.7.2.2-1
Seismic thrust	$T_{EQ} := \frac{\left(\frac{H}{ft}\right)^{0.6}}{\left(\frac{M_s}{ksi}\right)^{0.33}} \cdot 2 \cdot \frac{R}{ft} \cdot \frac{S}{ft} \cdot k_h \cdot \frac{lbf}{in}$	$T_{EQ} = 9.13 \cdot \frac{kip}{ft}$	
Design thrust Strength I Load Combination	$T_{S1} := 1.5 \cdot T_{DL} + 1.75 \cdot T_{LL}$	$T_{S1} = 22.23 \cdot \frac{kip}{ft}$	AASHTO Table 3.4.1-1
Design thrust Extreme Event I Load Combination	$T_{EE1} := 1.0 \cdot T_{DL} + 0.5 T_{LL} + 1.0 \cdot T_{EQ}$	$T_{EE1} = 22.54 \cdot \frac{kip}{ft}$	AASHTO Table 3.4.1-1
Thrust capacity	$T_n := 0.67 \cdot A_p \cdot f_y$	$T_n = 54.15 \cdot \frac{kip}{ft}$	AASHTO 12.7.2.3-1
			Thrust capacity is adequate.

APPENDIX C
Recommended AASHTO LRFD Modifications

3.10 – EARTHQUAKE EFFECTS: *EQ*

3.10.1 – General

Seismic effects for box culverts and buried structures need not be considered, except where ~~they~~ the structures cross active faults, where spans are greater than 20 ft and the structures impact life safety, or where required by local jurisdiction.

12.6 – GENERAL DESIGN FEATURES

12.6.1 – Loading

Earthquake loads should be considered only where buried structures cross active faults, where spans are greater than 20 ft and the structures impact life safety, or where required by local jurisdiction. When required, earthquake loads on corrugated metal long-span structural plate buried structures shall be calculated according to the provisions of Article 12.8.10.

12.8 – LONG-SPAN STRUCTURAL PLATE STRUCTURES

12.8.10 – Seismic Demands

12.8.10.1 – General

Eq. 12.8.10.2-1 and Eq. 12.8.10.3-1 are applicable only to installations meeting the requirements shown in Table 12.8.10.1-1. Installations not meeting these requirements require finite element analysis for the determination of seismic demands.

Table 12.8.10.1-1 – Applicability of Seismic Demand Equations

	Minimum	Maximum
Structure Span (ft)	20	60
Rise (ft)	10	40
Fill depth (ft)	2	10
Profile	6″x2″	15″x5.5″
Thickness (GA)	1	8
Structure Material	Steel, Aluminum	
Embedment Material	ML with 95% compaction or greater or SW with 85% compaction or greater	

C12.8.10.1

The proposed seismic demand equations were developed to give conservative estimates of demands due to seismic lateral accelerations calculated from detailed parametric finite element modeling (Ref XX). The applicability of the equations is limited to the range of study of the finite element models. Locations with faults, liquefaction, low-quality backfill, deep foundations,

structure slopes, or surface ground slopes should be evaluated using soil-structure interaction finite element analyses based on the specific site conditions.

Seismic demands are more likely to control design for installations with high seismicity, large structure span, deep cover, or poor native soil. The demand equations are expected to be especially conservative for installations with very good native soils, but seismic demands are unlikely to control for these cases.

See Article 11.6.5.2.1 for a discussion of seismic vertical accelerations. For cases where seismic vertical acceleration is considered significant, the force effects for vertical acceleration may be computed by scaling the dead load demands by a factor of $2/3*k_h$. Vertical and lateral seismic force effects should be combined per Article 3.10.8.

12.8.10.2 – Thrust

The factored seismic thrust in the wall shall be determined as:

$$T = \gamma_{EQ}\left(\frac{H^{0.6}}{{M_s}^{0.33}}\right) * 2 * R * S * k_h \qquad (12.8.10.2\text{-}1)$$

where:

T = factored seismic thrust (lbf/in.)
γ_{EQ} = load factor for seismic effects as specified in Article 3.4.1
H = fill depth (ft)
M_s = constrained modulus of native material (ksi) as specified in Table 12.12.3.5-1
R = structure rise (ft)
S = structure span (ft)
k_h = seismic lateral acceleration coefficient (g) as specified in Article 11.6.5.2.2

12.8.10.3 – Moment

The factored seismic moment in the wall shall be determined as:

$$M = \gamma_{EQ}\left(\frac{I * (R + 60)^4}{2975 * {M_s}^{0.1}} + 80\right) * k_h \qquad (12.8.10.3\text{-}1)$$

where:
M = factored seismic moment (lbf-in./in.)
γ_{EQ} = load factor for seismic effects as specified in Article 3.4.1
I = profile moment of inertia (in^4/in.)
R = structure rise (ft)
M_s = constrained modulus of native material (ksi) as specified in Table 12.12.3.5-1
k_h = seismic lateral acceleration coefficient (g) as specified in Article 11.6.5.2.2